

AD \_\_\_\_\_

AWARD NUMBER DAMD17-97-1-7195

TITLE: Determination of the Crystal Structure of Human Zn-Alpha 2-Glycoprotein, A Protein Implicated in Breast Cancer

PRINCIPAL INVESTIGATOR: Dr. Luis Sanchez  
Pamela J. Bjorkman, Ph.D.

CONTRACTING ORGANIZATION: California Institute of Technology  
Pasadena, California 91125

REPORT DATE: August 1999

TYPE OF REPORT: ANNUAL

PREPARED FOR: Commander  
U.S. Army Medical Research and Materiel Command  
Fort Detrick, Maryland 21702-5012

DISTRIBUTION STATEMENT: Approved for public release; distribution unlimited

The views, opinions and/or findings contained in this report are those of the author(s) and should not be construed as an official Department of the Army position, policy or decision unless so designated by other documentation.

DTIC QUALITY INSPECTED 4

20001017 055

# REPORT DOCUMENTATION PAGE

Form Approved  
OMB No. 0704-0188

Public reporting burden for this collection of information is estimated to average 1 hour per response, including the time for reviewing instructions, searching existing data sources, gathering and maintaining the data needed, and completing and reviewing the collection of information. Send comments regarding this burden estimate or any other aspect of this collection of information, including suggestions for reducing this burden, to Washington Headquarters Services, Directorate for Information Operations and Reports, 1215 Jefferson Davis Highway, Suite 1204, Arlington, VA 22202-4302, and to the Office of Management and Budget, Paperwork Reduction Project (0704-0188), Washington, DC 20503.

1. AGENCY USE ONLY <i>(Leave blank)</i>			2. REPORT DATE August 1999	
4. TITLE AND SUBTITLE  Determination of the Crystal Structure of Human Zn-Alpha 2-Glycoprotein, A Protein Implicated in Breast Cancer			3. REPORT Annual	
6. AUTHOR(S)  Dr. Luis Sanchez Pamela J. Bjorkman, Ph.D.			7. COVERED (1 Aug 98 - 31 Jul 99)	
7. PERFORMING ORGANIZATION NAME(S) AND ADDRESS(ES)  California Institute of Technology Pasadena, California 91125			8. FUNDING NUMBERS  DAMD17-97-1-7195	
9. SPONSORING / MONITORING AGENCY NAME(S) AND ADDRESS(ES)  U.S. Army Medical Research And Materiel Command ATTN: MCMR-RMI-S 504 Scott Street Fort Detrick, Maryland 21702-5012			10. SPONSORING / MONITORING AGENCY REPORT NUMBER	
11. SUPPLEMENTARY NOTES				
12a. DISTRIBUTION / AVAILABILITY STATEMENT  Approved for public release; distribution unlimited			12b. DISTRIBUTION CODE	
13. ABSTRACT <i>(Maximum 200 words)</i>  <p>Zn-<math>\alpha_2</math>-glycoprotein (ZAG) is a soluble protein that is present in serum and other body fluids. In addition, ZAG accumulates in breast cysts as well as in 40% of breast carcinomas. ZAG stimulates lipid degradation in adipocytes and causes the extensive fat losses associated with some advanced cancers. The 2.8 Å crystal structure of ZAG resembles a class I major histocompatibility complex (MHC) heavy chain, but ZAG does not bind the class I light chain <math>\beta_2</math>-microglobulin. The ZAG structure includes a large groove analogous to class I MHC peptide binding grooves. Instead of a peptide, the ZAG groove contains a non-peptidic compound that may be implicated in lipid catabolism under normal or pathological conditions.</p>				
14. SUBJECT TERMS  Breast Cancer <i>Cachexia</i> <i>MHC</i>			15. NUMBER OF PAGES 21	
			16. PRICE CODE	
17. SECURITY CLASSIFICATION OF REPORT  Unclassified	18. SECURITY CLASSIFICATION OF THIS PAGE  Unclassified	19. SECURITY CLASSIFICATION OF ABSTRACT  Unclassified	20. LIMITATION OF ABSTRACT  Unlimited	

FOREWORD

Opinions, interpretations, conclusions and recommendations are those of the author and are not necessarily endorsed by the U.S. Army.

Where copyrighted material is quoted, permission has been obtained to use such material.

Where material from documents designated for limited distribution is quoted, permission has been obtained to use the material.

Citations of commercial organizations and trade names in this report do not constitute an official Department of Army endorsement or approval of the products or services of these organizations.

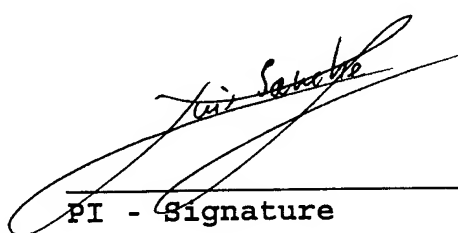
In conducting research using animals, the investigator(s) adhered to the "Guide for the Care and Use of Laboratory Animals," prepared by the Committee on Care and use of Laboratory Animals of the Institute of Laboratory Resources, national Research Council (NIH Publication No. 86-23, Revised 1985).

For the protection of human subjects, the investigator(s) adhered to policies of applicable Federal Law 45 CFR 46.

In conducting research utilizing recombinant DNA technology, the investigator(s) adhered to current guidelines promulgated by the National Institutes of Health.

In the conduct of research utilizing recombinant DNA, the investigator(s) adhered to the NIH Guidelines for Research Involving Recombinant DNA Molecules.

In the conduct of research involving hazardous organisms, the investigator(s) adhered to the CDC-NIH Guide for Biosafety in Microbiological and Biomedical Laboratories.

  
Tui Sato  
PI - Signature

24/9/1999  
Date

**Table of contents**

Front cover:	1
Report documentation page:	2
Foreword:	3
Table of contents:	4
Introduction:	5
Body:	6
Key research accomplishments:	8
Reportable outcomes:	9

## Introduction

Zn- $\alpha_2$ -glycoprotein (ZAG) is a soluble protein related to class I major histocompatibility complex proteins (MHC). ZAG is present in serum and other body fluids; in addition, it accumulates in breast cysts as well as in 40% of breast carcinomas. ZAG stimulates lipid degradation in adipocytes and causes the extensive fat losses associated with some advanced cancers. Our purpose is to determine the three-dimensional structure of ZAG. The information thus obtained will be the necessary basis for understanding the role of this protein in fat metabolism, as well as in breast cancer.

## Body

The only strategy capable to determine the structure of a macromolecule of 40 kDa, such as ZAG, is x-ray analysis of crystals of the macromolecule. Therefore, our first task was to obtain crystals of ZAG. The requirements for crystallizing a protein are 3-50 mgs of native protein that is both pure and conformationally homogeneous. We purified ZAG from human serum and eventually obtained crystals of the protein that were suitable for x-ray analysis.

Data obtained by crystallographic x-ray analysis are converted into a list of thousands of intensities. However, these intensities are not enough to solve the structure of macromolecules. Each intensity has to be complemented by an additional value, its “phase”, in order to reconstruct the image of the macromolecule. So, our next task was to obtain those phases. We estimated preliminary values for the phases by multiple isomorphous replacement (MIR). MIR is an experimental approach where protein crystals are soaked with different compounds containing heavy atoms. Comparison of x-ray data sets from soaked and non-soaked crystals can produce approximate values for the phases.

The image of the protein obtained by these studies is always blurred due to the inevitable errors in the measurements, particularly in the phases. We obtained this blurred image at the end of the previous research period. During the current research period, we have refined this image and built the atomic structure of ZAG inside it. Therefore, we have finally solved the three-dimensional structure of ZAG [1]. ZAG has a “L” shape in which the long axis of its  $\alpha_3$  domain is roughly perpendicular to the flat side of a platform formed by its  $\alpha_1$  and  $\alpha_2$  domains.

ZAG is the first known structure of a MHC-related protein that does not bind  $\beta_2$ -microglobulin ( $\beta_2$ M).  $\beta_2$ M is necessary for the correct folding of most MHC-related proteins and is tightly bound by the other domains of these

molecules. Later, the structure of another MHC-related protein that does not bind  $\beta_2$ M (MIC-A) was published [2] and shows severe distortions when compared with typical MHC molecules. However, ZAG remains folded in the absence of  $\beta_2$ M, and shows only minor rearrangements of its quaternary structure. Comparison of the interface between the  $\alpha_1$ - $\alpha_2$  platform and the  $\alpha_3$  domain reveals that an expanded hydrogen-bond network and an enlarged interdomain surface stabilize ZAG in the absence of  $\beta_2$ M.

The positions of some of the carbohydrates of ZAG are stabilized by crystal contacts. This fact allows the observation of nine residues in a biantennary structure, forming one of the biggest carbohydrate structures ever observed in a protein.

ZAG contains a large binding groove analogous to class I MHC peptide binding grooves. However, instead of a peptide, the ZAG groove contains a non-peptidic compound. This observation is perhaps the most important conclusion of this work, since it reveals that ZAG is a carrier of hydrophobic ligands that may be implicated in lipid catabolism and in the pathogenesis of breast cancer.

### References

1. Sánchez, L.M., A.J. Chirino, and P.J. Bjorkman, *Crystal structure of human ZAG, a fat-depleting factor related to MHC molecules*. Science, 1999. **283**(5409): p. 1914-9.
2. Li, P., et al., *Crystal structure of the MHC class I homolog MIC-A, a gammadelta T cell ligand*. Immunity, 1999. **10**(5): p. 577-84.

### Key research accomplishments

1. The structure of ZAG has been determined. I have learned protein crystallography and plan to use these skills to solve the three-dimensional structure of other proteins related to breast cancer.
2. The structure of ZAG reveals that this protein is a carrier of a hydrophobic non-peptidic ligand. I am using these results for identifying the ligand and planning mutagenesis experiments to characterize the function of ZAG in breast cancer and in the regulation of fat metabolism and body weight.
3. Comparison of the structures of ZAG and other members of the MHC family illuminates the role of  $\beta_2$ M in folding and stability, as well as the structural and functional differences between members that act as carriers of low molecular weight compounds and members that perform other functions.

### Reportable outcomes

Sánchez, L.M., A.J. Chirino, and P.J. Bjorkman, *Crystal structure of human ZAG, a fat-depleting factor related to MHC molecules*. *Science*, 1999. **283**(5409): p. 1914-9.

The results of this article have been commented in the Caltech Press Releases ([http://www.caltech.edu/~media/Press\\_Releases/PR11977.html](http://www.caltech.edu/~media/Press_Releases/PR11977.html)), and in the Howard Hughes Medical Institute News (<http://www.hhmi.org/news/bjorkman.htm>).

**Crystal Structure of Human  
ZAG, a Fat-Depleting Factor  
Related to MHC Molecules**

Luis M. Sánchez,<sup>1,\*</sup> Arthur J. Chirino,<sup>1,2,\*</sup> and Pamela J. Bjorkman<sup>1,2†</sup>

# Crystal Structure of Human ZAG, a Fat-Depleting Factor Related to MHC Molecules

Luis M. Sánchez,<sup>1</sup>\* Arthur J. Chirino,<sup>1,2</sup>\* Pamela J. Bjorkman<sup>1,2†</sup>

Zn- $\alpha_2$ -glycoprotein (ZAG) is a soluble protein that is present in serum and other body fluids. ZAG stimulates lipid degradation in adipocytes and causes the extensive fat losses associated with some advanced cancers. The 2.8 angstrom crystal structure of ZAG resembles a class I major histocompatibility complex (MHC) heavy chain, but ZAG does not bind the class I light chain  $\beta_2$ -microglobulin. The ZAG structure includes a large groove analogous to class I MHC peptide binding grooves. Instead of a peptide, the ZAG groove contains a nonpeptidic compound that may be implicated in lipid catabolism under normal or pathological conditions.

ZAG is a soluble protein whose name derives from its tendency to precipitate with zinc salts and its electrophoretic mobility in the region of the  $\alpha_2$  globulins (1). ZAG is normally present in most body fluids including serum, sweat, saliva, cerebrospinal fluid, seminal plasma, milk, amniotic fluid, and urine (1). In addition, ZAG accumulates in breast cysts as well as in 40% of breast carcinomas, and is induced by glucocorticoids and androgens in breast cancer cell lines. Hence, ZAG may participate in breast diseases, including cancer (2).

The function of ZAG was elucidated when a lipid-catabolizing factor with the same amino acid sequence as ZAG was isolated from the urine of cancer patients with cachexia (3). Cachexia is a wasting syndrome caused by depletion of muscle and adipose tissue that is present in the majority of patients with cancer, AIDS, and other life-threatening diseases (3). ZAG appears to be responsible for the fat-depletion component of cachexia, since it stimulates lipid breakdown in adipocytes and reduces fat stores in laboratory animals (3). ZAG is overexpressed in carcinomas that induce fat loss but not in other tumors. Application of ZAG to adipocyte membranes activates a guanosine triphosphate-dependent adenylate cyclase ac-

tivity, perhaps through direct or indirect interactions with a G protein-coupled receptor (3). Thus, its mode of action could be similar to that of lipolytic hormones. These results suggest that ZAG normally functions to regulate lipid degradation, which increases to a pathological extent in cachexia.

ZAG shares 30 to 40% amino acid sequence identity with the extracellular portions of class I major histocompatibility complex (MHC) heavy chains (4). Class I MHC molecules present peptide antigens to cytotoxic T cells (5). Other proteins related to class I MHC molecules include CD1, which presents hydrophobic antigens to T cells (6), the neonatal Fc receptor (FcRn), which transports immunoglobulin G across epithelia (7), and HFE, which binds transferrin receptor and regulates iron homeostasis (8). These MHC homologs are membrane-bound heterodimers that use the soluble protein  $\beta_2$ -microglobulin ( $\beta_2$ M) as a light chain. ZAG, however, is a secreted protein, and it does not associate with  $\beta_2$ M (9). The latter property is shared by MIC-A, a divergent membrane-bound member of the class I family (10).

Like FcRn (11), HFE (11), and MIC-A (10), ZAG does not bind endogenous peptides (9), but it appears to carry a small proteinase-resistant compound whose injection induces glomerulonephritis in experimental animals (12). In peptide-binding class I MHC molecules, a large groove located between two  $\alpha$  helices in the  $\alpha 1$ - $\alpha 2$  superdomain of the heavy chain serves as the binding site (5). An analogous groove acts as the antigen binding site in CD1,

<sup>1</sup>Division of Biology 156-29 and <sup>2</sup>Howard Hughes Medical Institute, California Institute of Technology, Pasadena, CA 91125, USA.

\*These authors contributed equally to this work.

†To whom correspondence should be addressed. E-mail: bjorkman@cco.caltech.edu

but is narrowed in HFE and closed in FcRn, the class I-related proteins that do not bind small molecular weight ligands (11).

Here, we present the 2.8 Å crystal structure of human ZAG, which reveals an MHC-like fold without a  $\beta_2$ M light chain and a

groove that closely resembles the peptide-binding sites of classical class I MHC molecules. Rather than containing a peptide, the

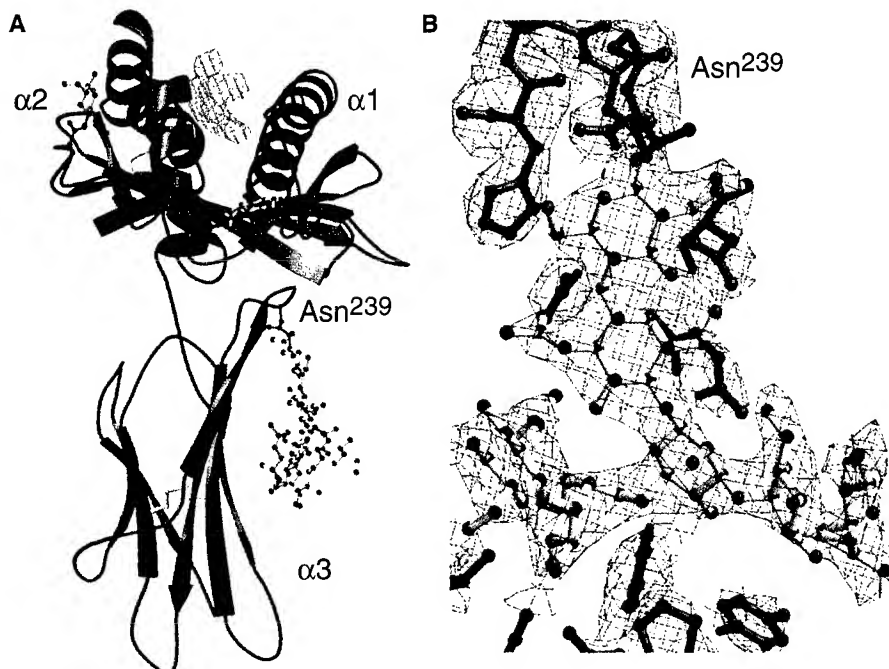


**Table 1.** Data collection, heavy-atom phasing, and refinement statistics for ZAG. Statistics in parentheses refer to the highest resolution bin. ZAG was crystallized in space group  $P2_12_12$  with four molecules per asymmetric unit and cryoprotected as described (9). Native and heavy-atom derivative data sets were collected at  $-165^\circ\text{C}$  from multiple crystals using an R-AXIS IIc imaging plate system mounted on a Rigaku R200 rotating anode generator.

Data set	Resolution (Å)	Complete (%)*	$R_{\text{merge}}\text{ (%)}\dagger$	$I/\sigma I$	$\text{rms } f_h/E \ddagger$
Native I	2.9	97.0 (83.0)	10.7 (29.7)	27.9 (3.2)	
Native II	2.8	96.0 (76.0)	6.6 (45.3)	24.7 (2.5)	
Mercury acetate					
1	3.4	94.4 (97.5)	13.6 (30.4)	10.8 (4.4)	3.0
2	4.0	94.4 (97.2)	17.9 (35.5)	6.8 (3.3)	2.2
3	3.4	98.5 (99.1)	13.2 (32.4)	9.9 (3.9)	2.8
4	3.2	97.7 (93.3)	7.8 (30.8)	19.1 (4.3)	1.9
PIP§					
1	3.7	91.8 (77.3)	5.7 (35.4)	22.1 (3.5)	1.1
2	3.2	98.5 (97.7)	7.3 (33.6)	22.0 (4.1)	0.8
3	3.6	95.4 (96.4)	8.1 (29.5)	20.8 (5.2)	1.0
$\text{K}_2\text{PtCl}_4$	4.0	98.8 (99.3)	13.0 (39.5)	10.1 (3.1)	1.5

Data were processed and scaled with the HKL package (13). Heavy-atom refinement was done with SHARP (13), which treated different data sets of derivatives with the same sites as separate "crystals" of the same "compound" and refined separate heavy-atom occupancies and temperature factors for each "crystal" data set. Electron density maps calculated from MIRAS phases derived from all eight heavy-atom data sets were superior to maps derived from various combinations of mercury and platinum data sets. Eight NCS operators were determined from least squares superposition of HLA-A2  $\alpha_1$ - $\alpha_2$  and  $\alpha_3$  domains manually placed in the electron density, four relating the  $\alpha_1$ - $\alpha_2$  regions and four relating the  $\alpha_3$  domains. After solvent flipping using Solomon (13), subdomain NCS averaging of the four molecules and phase extension from 5.0 to 2.9 Å were carried out with DM in the CCP4 suite (13) (final average correlation  $>0.8$ ). When the same averaging and phase extension procedure was done without prior solvent flipping, the resulting electron density maps were inferior. The model was built using O (13) and refined as described (13).

Refinement statistics					
Resolution (Å)		20.0–2.8	rms $\Delta B$ bonded NCS atoms (Å²) #		14.4, 15.4, 19.0
Reflections in working set	$ F  > 0$	37148	rms $\Delta \phi$ all NCS residues (degrees) #		2.4, 3.2, 3.7
Reflections in test set	$ F  > 0$	1970	rms $\Delta \psi$ all NCS residues (degrees) #		2.0, 2.3, 2.4
$R_{\text{free}}\text{ (%)}\parallel$		28.8	Number of nonhydrogen atoms		
$R_{\text{cryst}}\text{ (%)}\parallel$		22.9	Protein	8866	
rms deviations from ideal			Carbohydrate	388	
Bond lengths (Å)		0.008	Nonglycine residues in allowed		
Bond angles (degrees)		1.35	regions of Ramachandran plot as defined (13)	96%	

\*Complete = (number of independent reflections)/total theoretical number. † $R_{\text{merge}}\text{ (I)} = [\sum |I(i)| - \langle I(h) \rangle] / \sum |I(i)|$ , where  $I(i)$  is the  $i$ th observation of the intensity of the hkl reflection and  $\langle I \rangle$  is the mean intensity from multiple measurements of the hkl reflection. ‡rms  $f_h/E$  (phasing power), where  $f_h$  is the heavy-atom structure factor amplitude and  $E$  is the residual lack of closure error. §PIP, di-m-iodobis(ethylene diamine)diplatinum nitrate. || $R_{\text{free}}$  is calculated over reflections in a test set not included in atomic refinement. ¶ $R_{\text{cryst}}\text{ (F)} = \sum_h |F_{\text{obs}}(h)| - |F_{\text{calc}}(h)| / \sum_h |F_{\text{obs}}(h)|$ , where  $|F_{\text{obs}}(h)|$  and  $|F_{\text{calc}}(h)|$  are the observed and calculated structure factor amplitudes for the hkl reflection. #Statistics for NCS-related residues refer to differences relative to molecule 1 for the other three molecules in the crystallographic asymmetric unit.

ZAG groove includes an unidentified non-peptidic ligand that may be relevant for ZAG's function in lipid catabolism.

ZAG was purified from human serum and crystallized as described (9). The crystal structure was determined by multiple isomorphous replacement with anomalous scattering (MIRAS) aided by fourfold noncrystallographic symmetry (NCS) averaging (Table 1) (13). The overall structure of ZAG is similar to those of class I MHC heavy chains (Fig. 1A). The  $\alpha 1$ - $\alpha 2$  superdomains of ZAG, class I, and class I-related proteins form a single eight-stranded antiparallel  $\beta$  sheet topped by two  $\alpha$  helices, and the  $\alpha 3$  domain adopts a fold resembling immunoglobulin constant domains (5, 11). Electron density corresponding to carbohydrate is present at three of the four potential N-linked glycosylation sites in ZAG, with an unusually large number of ordered carbohydrate residues visible at Asn<sup>239</sup> (Fig. 1B) (14). The  $\alpha 3$  domain of human, but not mouse or rat, ZAG contains an RGD sequence (Arg<sup>231</sup>, Gly<sup>232</sup>, Asp<sup>233</sup>) suggested to be involved in cell adhesion (15). However, unlike the RGD sequences in characterized adhesion molecules such as fibronectin III domains (15), the ZAG RGD is located in a  $\beta$  strand rather than a loop.

The quaternary arrangement of the ZAG  $\alpha 3$  domain with respect to the  $\alpha 1$ - $\alpha 2$  platform differs from that found in  $\beta_2$ M-binding class I and class I-related proteins. The overall shape of ZAG is similar to an inverted "L," in which the long axis of the  $\alpha 3$  domain is roughly perpendicular to the flat side of the  $\alpha 1$ - $\alpha 2$  platform, whereas the comparable angle is acute in  $\beta_2$ M-binding proteins (Fig. 2A). In those proteins,  $\beta_2$ M interacts with the  $\alpha 3$  domain and the underside of the  $\alpha 1$ - $\alpha 2$  platform and is typically required for stability (16). The displacement of the ZAG  $\alpha 3$  domain compared to its class I counterpart results in the inability of  $\beta_2$ M to optimally contact the  $\alpha 3$  and  $\alpha 1$ - $\alpha 2$  domains of ZAG (17), contributing to ZAG's lack of affinity for  $\beta_2$ M. The high thermal stability of ZAG in the absence of  $\beta_2$ M (9) can be explained by a network of hydrogen bonds between  $\alpha 3$  and  $\alpha 1$ - $\alpha 2$  that are not present in  $\beta_2$ M-binding class I proteins (Fig. 2B). In addition to the extra hydrogen bonds, the loop connecting  $\beta$  strand 4 to the helical region of the ZAG  $\alpha 1$  domain platform (residues 51 to 54) and the loop connecting strands D to E in the  $\alpha 3$  domain (residues 236 to 241) are closer together than their class I counterparts, contributing to the burial of a larger interdomain surface in ZAG (970 Å<sup>2</sup> total) than in classical class I molecules (660 Å<sup>2</sup> in HLA-A2) (11). There is some flexibility in the position of the ZAG  $\alpha 3$  domain relative to  $\alpha 1$ - $\alpha 2$ , as demonstrated by different interdomain relationships of the four ZAG molecules in the crystallographic asymmetric unit (Fig. 2A), yet ZAG is not particularly protease-sensitive at the platform-

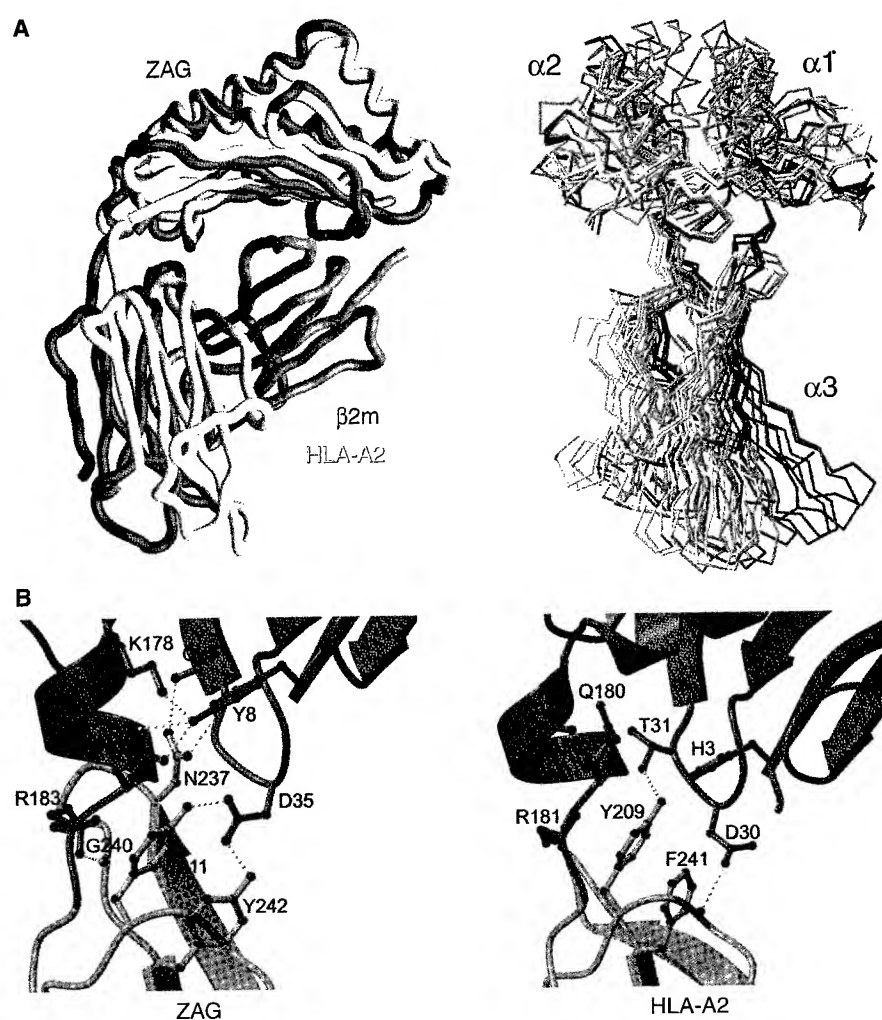


**Fig. 2.** Structural comparisons of ZAG, class I, and class I-related proteins. (A) (Left) Comparison of the structures of ZAG and HLA-A2 (11). (Right) Comparison of the four ZAG molecules in the crystallographic asymmetric unit (magenta) with the heavy chains of human class I MHC (yellow; PDB codes 1hhh, 1vac, 2clr) and  $\beta_2$ M-binding class I MHC homologs (green; FcRn, CD1, HFE) (11). Superpositions were based on the  $\text{C}\alpha$  atoms in the platform domains, using 2clr as a reference molecule. The position of the ZAG  $\alpha 3$  domain with respect to its  $\alpha 1$ - $\alpha 2$  platform falls out of the range of the positions of the  $\alpha 3$  domains of the  $\beta_2$ M-binding class I proteins. Differences in the platform- $\alpha 3$  interdomain relationships in the four ZAG molecules demonstrate that there is flexibility in the position of the ZAG  $\alpha 3$  domain relative to  $\alpha 1$ - $\alpha 2$ . However, the overall similarity of the four molecules, which are subjected to different crystal packing forces, rule out that ZAG's shape is an artifact of crystallization. (B) Close-up comparison of the interface between  $\alpha 1$ - $\alpha 2$  (blue) and  $\alpha 3$  (green) in ZAG and HLA-A2 (11). Additional H-bonds and a larger interdomain surface area stabilize ZAG compared with class I molecules, whose heavy chains are stabilized by interactions with  $\beta_2$ M. Figures were made as described (23).

$\alpha 3$  hinge or any other region (18). Although the quaternary structure of ZAG differs significantly from the heavy chains of class I and class I-like structures, the differences are less than anticipated from the absence of the  $\beta_2$ M light chain. The overall similarity between ZAG and class I MHC heavy chains contrasts with the large interdomain rearrangements observed in the crystal structure of MIC-A (10).

Despite the similarity between ZAG and class I molecules, structural features of the ZAG  $\alpha 3$  domain make it unlikely to associate with the T cell coreceptor CD8. Of 15 class I heavy-chain residues identified at the CD8 binding site in the HLA-A2/CD8 cocrystal

structure (19), only one is conserved between class I and ZAG sequences (class I Asp<sup>122</sup>, ZAG Asp<sup>123</sup>) (4). It is not possible to rule out an interaction between ZAG and T cell receptors, because the class I MHC residues that contact these receptors are not particularly conserved (20).

Although ZAG does not associate with peptides (9), the helices in both the  $\alpha 1$  and  $\alpha 2$  domains are almost identically positioned to their counterparts in peptide-binding class I MHC molecules (Fig. 3A) (21). Thus, the ZAG platform includes an open groove, by contrast to the narrowed or closed grooves observed in other class I homologs that do not bind peptides

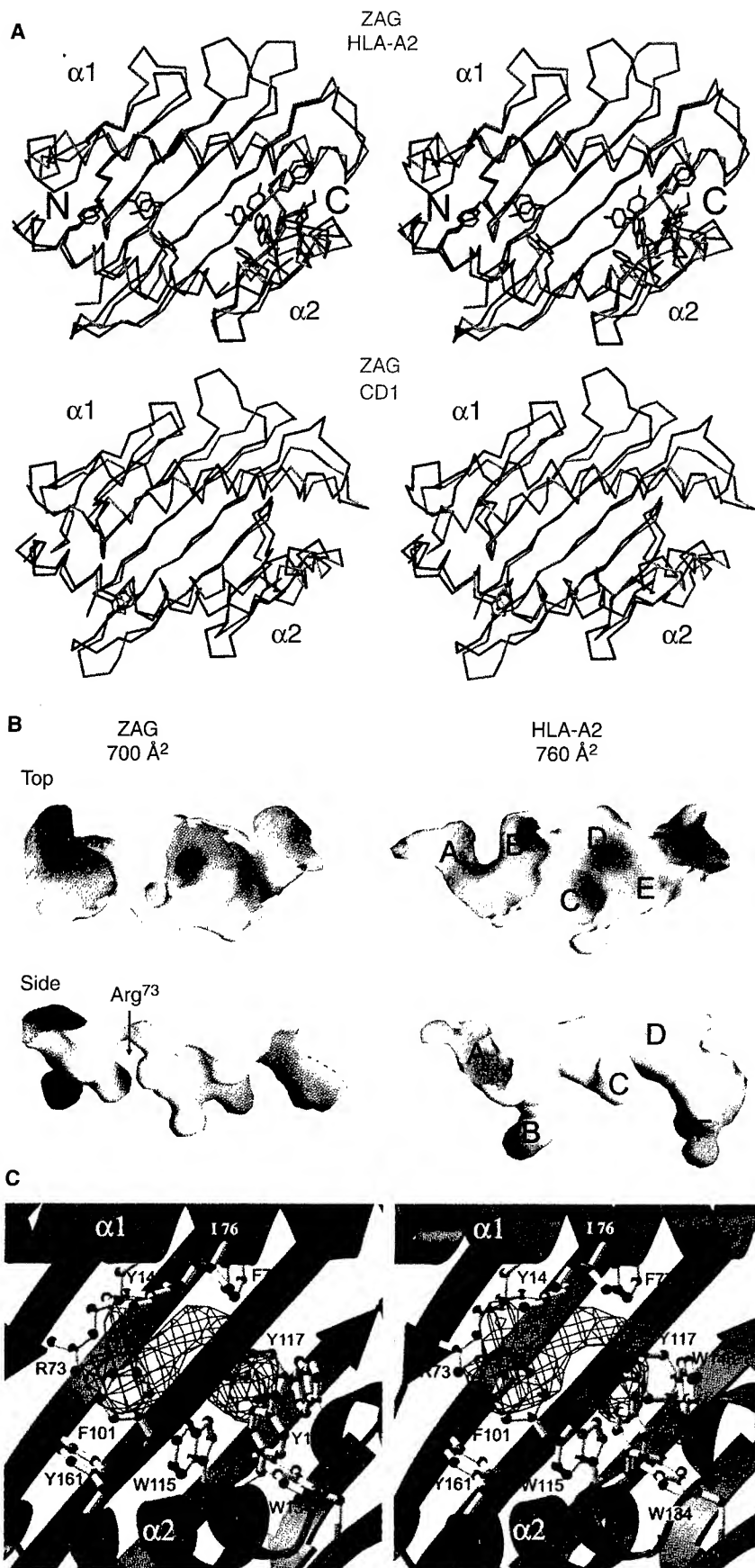


**Fig. 3. Comparisons of the grooves of ZAG, class I, and class I-related proteins. (A)** Stereoview comparisons of the  $\alpha_1$ - $\alpha_2$  platforms of ZAG and class I proteins that contain open antigen-binding grooves. (Top) ZAG is compared with HLA-A2, a classical class I MHC molecule. "N" and "C" indicate the orientation with respect to the  $\text{NH}_2$ - and  $\text{COOH}$ -termini of a peptide bound in the HLA-A2 groove. Side chains in common between the ZAG and HLA-A2 grooves (Table 2) are highlighted on the  $\text{C}\alpha$  backbones. Although many of the ZAG groove residues are chemically identical to their counterparts in HLA-A2, the conformations of the side chain, the backbone, or both, of these residues are generally different; thus, the grooves have different shapes [see (B)]. (Bottom) Comparison of ZAG and CD1. Although the ZAG and CD1 grooves both bind nonpeptidic ligands, the ZAG groove is smaller and shallower. Prolines within the  $\alpha_2$  domain helices of ZAG (Pro<sup>167</sup>) and CD1 (Pro<sup>169</sup>) are highlighted. The proline in the ZAG helix is accommodated without significant distortion (24), as previously seen for the analogous proline within the HFE helix (Pro<sup>166</sup>) (11). (B) Extruded groove pockets of ZAG and HLA-A2. Cutaway groove molecular surfaces (11) are shown from above (top) and the side (bottom) with electrostatic potentials (23), in which positive potential is blue, neutral is white, and negative potential is red. The approximate locations of pockets A through F (Table 2) are indicated on the HLA-A2 surfaces. The molecular surface of the central portion of the ZAG groove is nearly neutral except for the contribution of Arg<sup>73</sup> and, like CD1 (11), is hydrophobic compared to the grooves of the class I molecules. Calculated groove surface areas (11) are indicated for ZAG and HLA-A2. For comparison, the groove surface areas for other MHC homologs are  $\sim 1440$  Å<sup>2</sup> (CD1),  $\sim 235$  Å<sup>2</sup> (FcRn), and  $\sim 415$  Å<sup>2</sup> (HFE) (11). (C) Stereoview of electron density (from a 2.9 Å MIRAS, NCS averaged, figure-of-merit weighted electron density map contoured at  $1\sigma$ ) corresponding to the ZAG ligand superimposed upon a ribbon diagram of the ZAG  $\alpha_1$ - $\alpha_2$  platform. Residues within 4.5 Å of the density (Table 2) are highlighted in ball-and-stick representation. Figures were made as described (23).

[FcRn (11), HFE (11), and MIC-A (10)]. Despite the fact that most of the residues within the COOH-terminal portion of the ZAG  $\alpha$ 2 domain helix are chemically identical to their class I counterparts (Table 2), the ZAG groove has a different shape than a typical class I MHC peptide-binding groove (Fig. 3B). Differences in side chain conformations (Fig. 3A) and side chain substitutions create the altered shape of the ZAG groove, which can be described as containing three pockets: a large, predominantly hydrophobic central pocket and two smaller, more acidic flanking pockets (Fig. 3B). The boundary on the left of the central pocket (Fig. 3B) is created by the side chain of Arg<sup>73</sup>, which points into the groove to separate the central and left pockets. Class I MHC grooves contain a smaller side chain at this position (His<sup>70</sup> in

HLA-A2) (4). Because of Arg<sup>73</sup> and other side chain substitutions or conformational differences relative to class I molecules, the ZAG groove cannot accommodate even a polyalanine version of an eight- or nine-residue peptide in a class I-binding conformation (Table 2).

Instead of a peptide, the ZAG groove contains an as yet unidentified ligand that cocrystallizes with the protein. Electron density that cannot be accounted for by the amino acid sequence or N-linked carbohydrates is found in the central pocket of the ZAG groove (Figs. 1A and 3C). The density is a curved nonbranched tube, lacking the characteristic protrusions of peptides, that is situated near a cluster of hydrophobic amino acids (three tryptophans, four tyrosines, an isoleucine, and two phenylalanines) and the positively charged side chain of

Arg<sup>73</sup> (Table 2). Although it is not possible to unambiguously identify the compound or compounds in the ZAG groove at the current resolution of the electron density maps, previous biochemical studies rule out that the density corresponds to peptide or mixture of peptides (9). The composition of the ZAG groove residues near the density (Table 2) suggests that it represents one or more small hydrophobic molecules, perhaps negatively charged. Chloroform-methanol extractions and acid eluates of ZAG as well as the intact protein have been analyzed by gas chromatography, electrospray, or matrix-assisted laser desorption/ionization mass spectrometry, or a combination of these methods (22). The ligand has not yet been detected, but in the absence of information about the chemical nature, size, and ionic state of the ligand, these results cannot be considered conclusive. Electrospray analyses of proteolytic fragments of ZAG reveal that the ligand is not covalently bound (22).

Classical class I MHC molecules are extremely polymorphic, whereas ZAG exhibits species-specific variations but little or no genetic polymorphism (4, 5). Most of the allele-specific variations of class I MHC molecules map to residues within the peptide-binding groove that interact with peptides (Table 2) (5). This property of class I molecules results in allele-specific peptide-binding motifs, such that individual class I molecules show distinct preferences for binding peptides (5). In contrast, residues within the ZAG groove are mostly conserved, and those residues closest to the ZAG ligand are completely conserved (Table 2), even though human and rodent ZAG share only ~56% sequence identity (4). Taken together with ZAG's lack of polymorphism, these observations imply that human and rodent ZAG carry a single compound, or single class of compounds, related to their function in lipid catabolism.

The crystallographic analysis of ZAG reveals a structure with surprising similarity to classical class I molecules despite ZAG's inability to bind peptides or  $\beta_2$ M (9). ZAG and MHC-related proteins such as FcRn (11) and HFE (11) have adapted the same basic fold to perform widely different roles within and outside of the immune system. These molecules illustrate the versatility of the MHC fold and raise intriguing questions about the ancestral function and evolutionary relationships of MHC and MHC-related proteins.

#### References and Notes

1. W. Bürgi and K. Schmid, *J. Biol. Chem.* **236**, 1066 (1961); T. Tada et al., *J. Histochem. Cytochem.* **39**, 1221 (1991).
2. N. J. Bundred, W. R. Miller, R. A. Walker, *Histopathology* **11**, 603 (1987); J. P. Freije, A. Fueyo, J. Uría, C. López-Otín, *FEBS Lett.* **290**, 247 (1991); L. M. Sánchez, F. Vizoso, I. Díez-Itza, C. López-Otín, *Cancer Res.* **52**, 95 (1992); I. Díez-Itza et al., *Eur. J. Cancer* **29**, 1256 (1993); Y. S. López-Boado, I. Díez-Itza, J. Tolivia, C. López-Otín, *Breast Cancer Res. Treat.* **29**, 247 (1994).

**Table 2.** Comparison of residues in  $\alpha$ 1- $\alpha$ 2 grooves of ZAG and a class I MHC molecule. Uppercase letters in any of the HLA-A2 and ZAG columns indicate residues that are conserved in human class I MHC sequences (4) or residues that are conserved in human, mouse, and rat ZAG (4). Pocket residues in the peptide-binding groove of HLA-A2 are defined as having  $\geq 5.0 \text{ \AA}^2$  accessible surface area to a  $1.4 \text{ \AA}$  probe, but  $< 5.0 \text{ \AA}^2$  accessible surface area to a  $5 \text{ \AA}$  probe (11). HLA-A2 residues marked with an asterisk were originally defined as pocket residues by M. A. Saper et al. (11) but are accessible to a  $5.0 \text{ \AA}$  probe. The HLA-A2 residues designated as "NONE" (conserved) or "none" (not conserved) do not meet the criteria for being in a pocket, but are listed for comparison with ZAG. Pocket letter names (uppercase letters, conserved residues) refer to well-characterized pockets in the peptide-binding grooves of class I MHC molecules (5, 11). ZAG residues analogous to class I pocket residues are designated as "POCKET" (conserved) or "pocket" (not conserved) if they meet the criteria for pocket residues in HLA-A2, "BURIED" or "buried" if they have  $\leq 5.0 \text{ \AA}^2$  accessible surface area to a  $1.4 \text{ \AA}$  probe and  $\leq 5.0 \text{ \AA}^2$  accessible surface area to a  $5 \text{ \AA}$  probe, and "EXPOSED" or "exposed" if they have  $\geq 5.0 \text{ \AA}^2$  accessible surface area to a  $1.4 \text{ \AA}$  probe and  $\geq 5.0 \text{ \AA}^2$  accessible surface area to a  $5 \text{ \AA}$  probe. Surface areas were calculated (11) using the coordinates of HLA-A2 (excluding water molecules and bound peptide) and ZAG. Steric clashes with polyalanine peptides bound to ZAG in their class I-binding configuration were defined as described in the structural analysis of HFE (11).

HLA-A2	Pocket	ZAG	Pocket	Clash with peptide?	$\leq 4.5 \text{ \AA}$ of ZAG ligand?
MET-5	A	LEU-10	BURIED	NO	NO
TYR-7	A,B	tyr-12	pocket	yes	no
phe-9	b,c	TYR-14	POCKET	NO	YES
met-45	b	ser-48	pocket	no	no
tyr-59	a	ASP-62	EXPOSED	NO	NO
glu-63	a,b	asp-66	pocket	no	no
lys-66*	a	LEU-69	EXPOSED	YES	NO
val-67	b	GLN-70	POCKET	YES	NO
his-70	b,c	ARG-73	POCKET	YES	YES
thr-73*	c	ILE-76	EXPOSED	YES	YES
his-74	none	PHE-77	POCKET	NO	YES
val-76	none	glu-79	exposed	yes	no
asp-77*	f	THR-80	POCKET	YES	NO
thr-80*	f	ASP-83	EXPOSED	YES	NO
leu-81	f	ILE-84	POCKET	NO	NO
arg-97	c,e	GLY-99	POCKET	NO	NO
tyr-99	a,b,c,d	PHE-101	POCKET	NO	YES
his-114	c,d,e	TRP-115	POCKET	NO	YES
tyr-116	c,f	TYR-117	POCKET	NO	YES
TYR-118	F	TYR-119	POCKET	NO	NO
TYR-123	F	tyr-124	pocket	no	no
ILE-124	F	ILE-125	BURIED	NO	NO
TRP-133	NONE	TRP-134	POCKET	NO	YES
thr-143	f	THR-144	POCKET	YES	NO
LYS-146	NONE	LYS-147	EXPOSED	YES	NO
trp-147	e,f	TRP-148	POCKET	NO	YES
val-152	e	TYR-154	EXPOSED	NO	YES
leu-156	d,e	ALA-158	POCKET	NO	NO
TYR-159	A,D	TYR-161	POCKET	YES	YES
trp-167	a	thr-169	pocket	yes	no
tyr-171	a	TYR-173	POCKET	YES	NO

3. P. T. Todorov *et al.*, *Cancer Res.* **58**, 2353 (1998); K. Hirai, H. J. Hussey, M. D. Barber, S. A. Price, M. J. Tisdale, *ibid.*, p. 2359.

4. Protein sequences: Human ZAG [T. Araki *et al.*, *Proc. Natl. Acad. Sci. U.S.A.* **85**, 679 (1988)]; mouse ZAG [H. Ueyama, H. Naitoh, I. Ohkubo, *J. Biochem.* **116**, 677 (1994)]; rat ZAG [A. Fueyo, J. A. Uri, J. P. Freije, C. López-Otín, *Gene* **145**, 245 (1994)]. Human class I MHC sequences [P. J. Bjorkman and P. Parham, *Annu. Rev. Biochem.* **59**, 253 (1990)]; MHC homolog sequences, SWISS-PROT [A. Bairoch and R. Apweiler, *Nucleic Acids Res.* **26**, 38 (1998)]. Sequence identities: ZAG and HLA-A2, 36%; ZAG and FcRn, 27%; ZAG and mouse CD1d, 23%; ZAG and HFE, 36%; ZAG and MIC-A, 29%.

5. D. R. Madden, *Annu. Rev. Immunol.* **13**, 587 (1995).

6. E. M. Beckman *et al.*, *Nature* **372**, 691 (1994); A. R. Castaño *et al.*, *Science* **269**, 223 (1995).

7. R. P. Junghans, *Immunol. Res.* **16**, 29 (1997); V. Ghetie and E. S. Ward, *Immunol. Today* **18**, 592 (1997); N. E. Simister, E. J. Israel, J. C. Ahouse, C. M. Story, *Biochem. Soc. Trans.* **25**, 481 (1997).

8. J. N. Feder *et al.*, *Nature Genet.* **13**, 399 (1996); J. N. Feder *et al.*, *Proc. Natl. Acad. Sci. U.S.A.* **93**, 1472 (1996).

9. L. M. Sánchez, C. López-Otín, P. J. Bjorkman, *Proc. Natl. Acad. Sci. U.S.A.* **94**, 4626 (1997). In thermal denaturation studies, ZAG denatures with a transition midpoint of 65°C, compared to 57°C for the peptide-filled class I molecule H-2K<sup>d</sup> and 45°C for empty K<sup>d</sup> [M. L. Fahnestock, I. Tamir, L. Narhi, P. J. Bjorkman, *Science* **258**, 1658 (1992)].

10. V. Groh *et al.*, *Proc. Natl. Acad. Sci. U.S.A.* **93**, 12445 (1996). The crystal structure of MIC-A reveals a major rearrangement in domain organization compared to the structures of class I molecules and ZAG. The MIC-A  $\alpha$ 1- $\alpha$ 2 platform is displaced from its  $\alpha$ 3 domain by 113.5° compared to class I molecules. As a result, the MIC-A  $\alpha$ 1- $\alpha$ 2 platform makes no contact with its  $\alpha$ 3 domain [P. Li, S. T. Willie, S. Bauer, D. L. Morris, T. Spies, R. K. Strong, personal communication].

11. Protein structures: HLA-A2 [Protein Data Bank (PDB) code 2CLR] [E. J. Collins, D. N. Garboczi, D. C. Wiley, *Nature* **371**, 626 (1994)]; Mouse CD1 (PDB code 1CD1) [Z.-H. Zeng *et al.*, *Science* **277**, 339 (1997)]; Rat FcRn (PDB code 3FRU) [W. P. Burmester, L. N. Gatinet, N. E. Simister, M. L. Blum, P. J. Bjorkman, *Nature* **372**, 336 (1994)]; Human HFE (PDB code 1A6Z) [J. A. Lebrón *et al.*, *Cell* **93**, 111 (1998)]. Molecular surface areas buried by interaction were calculated with X-PLOR [A. T. Brünger, *X-PLOR. Version 3.1: A System for X-ray and NMR* (Yale Univ. Press, New Haven, CT, 1992)] with a 1.4 Å radius. Identification of pocket residues and calculation of groove surface areas were done based upon earlier analyses of human and mouse class I structures [M. A. Saper, P. J. Bjorkman, D. C. Wiley, *J. Mol. Biol.* **219**, 277 (1991); M. Matsumura, D. H. Fremont, P. A. Peterson, I. A. Wilson, *Science* **257**, 927 (1992)] as described in the CD1 (Z.-H. Zeng *et al.*) and HFE (J. A. Lebrón *et al.*) structure papers. Cut away molecular surfaces of grooves (Fig. 3B) were generated as described in the CD1 structure paper.

12. S. Shibata and K. Miura, *Nephron* **31**, 170 (1982).

13. Structure determination and refinement: HKL [Z. Otwowski and W. Minor, *Methods Enzymol.* **276**, 307 (1997)]; SHARP [E. De La Fortelle and G. Bricogne, *ibid.*, p. 472]; Solomon [J. P. Abrahams and A. G. W. Leslie, *Acta Crystallogr. D* **52**, 30 (1996)]; CCP4 programs [CCP4: Collaborative Computational Project No. 4, Daresbury, UK, *Acta Crystallogr. D* **50**, 760 (1994)]. O [T. A. Jones and M. Kjeldgaard, *Methods Enzymol.* **277**, 173 (1997)],  $R_{\text{free}}$  [A. T. Brünger, *Nature* **355**, 472 (1992)]. The Native II data set (Table 1) was used for refinement. After rigid-body refinement of eight domains in the asymmetric unit ( $\alpha$ 1- $\alpha$ 2 and  $\alpha$ 3 for each of four ZAG molecules) using CNS [A. T. Brünger *et al.*, *Acta Crystallogr. D* **54**, 905 (1998)], the four molecules were subjected to restrained NCS torsion-angle refinement using the maximum likelihood target function. Tight NCS restraints (300 kcal/mol·Å<sup>2</sup>) were applied to all regions except for flexible loops and residues involved in lattice contacts. Intermediate rounds of model building and refinement included the calculation of SIGMA-weighted [R. J. Read, *Acta Crystallogr. A* **42**, 140 (1986)] simulated annealing omit maps [A. Hodel, S.-H. Kim, A. T. Brünger, *Acta Crystallogr. A* **48**, 851 (1992)]. Final rounds of rebuilding and refinement included tightly restrained individual atomic temperature factor refinement (temperature factor rms deviation for bonded main chain and side chain atoms is 5.7 and 8.8 Å<sup>2</sup>, respectively). The model consists of residues 5 through 277 (average  $B$ : 48 Å<sup>2</sup>) with nine carbohydrate residues (average  $B$ : 61 Å<sup>2</sup>) for molecule 1, residues 5 through 278 (average  $B$ : 56 Å<sup>2</sup>) with 11 carbohydrate residues (average  $B$ : 80 Å<sup>2</sup>) for molecule 2, residues 6 through 278 (average  $B$ : 57 Å<sup>2</sup>) with four carbohydrate residues (average  $B$ : 107 Å<sup>2</sup>) for molecule 3, and residues 6 through 249 and 258 through 276 (average  $B$ : 62 Å<sup>2</sup>) with five carbohydrate residues (average  $B$ : 90 Å<sup>2</sup>) for molecule 4 (Wilson  $B$  = 64 Å<sup>2</sup>). Excluding regions that deviate from the NCS, the domains in the NCS-related ZAG monomers are very similar (<0.04 Å rms deviation for C $\alpha$  atoms). Ramachandran plot statistics (Table 1) are as defined by G. J. Kleywegt and T. A. Jones [*Structure* **4**, 1395 (1996)].

14. Extensive carbohydrate density is found at Asn<sup>239</sup> (nine ordered carbohydrate residues in molecule 2) and to a much lesser extent at Asn<sup>89</sup> and Asn<sup>108</sup> in all four ZAG molecules (Fig. 1) (13). Crystal structures of glycoproteins rarely show more than three ordered carbohydrate residues at each glycosylation site [D. E. Vaughn and P. J. Bjorkman, *Structure* **6**, 63 (1998)]. The Asn in the fourth potential N-linked glycosylation site (Asn<sup>92</sup>) does not show density corresponding to carbohydrate. The bond between Asn<sup>92</sup> and Gly<sup>93</sup> can be cleaved by hydroxylamine, confirming that Asn<sup>92</sup> is not glycosylated (18).

15. M. Takagaki *et al.*, *Biochem. Biophys. Res. Commun.* **201**, 1339 (1994); O. Ogikubo *et al.*, *ibid.* **252**, 257 (1998); M. Pfaff, in *Integrin-Ligand Interaction*, J. A. Eble and K. Kühn, Eds. (Chapman & Hall, New York, 1997), pp. 101–121.

16. V. A. Tysoe-Calnon, J. E. Grundy, S. J. Perkins, *Biochem. J.* **277**, 359 (1991); D. Lancet, P. Parham, J. L. Strominger, *Proc. Natl. Acad. Sci. U.S.A.* **76**, 3844 (1979); A. Bauer *et al.*, *Eur. J. Immunol.* **27**, 1366 (1997).

17. Structural features that prevent ZAG from binding  $\beta_2$ M include the following residues, which clash with  $\beta_2$ M when it is positioned on the ZAG structure either by interacting with  $\alpha$ 3 or with  $\alpha$ 1- $\alpha$ 2: Ile<sup>13</sup>, Thr<sup>15</sup>, Leu<sup>30</sup>, Arg<sup>40</sup>, Gln<sup>98</sup>, Tyr<sup>118</sup>, Lys<sup>122</sup>, Val<sup>234</sup>, His<sup>236</sup>, Trp<sup>245</sup>.

18. L. M. Sánchez and P. J. Bjorkman, unpublished results.

19. G. F. Gao *et al.*, *Nature* **387**, 630 (1997).

20. D. N. Garboczi *et al.*, *ibid.* **384**, 134 (1996); K. C. Garcia *et al.*, *Science* **274**, 209 (1996); Y. H. Ding *et al.*, *Immunity* **8**, 403 (1998); K. C. Garcia *et al.*, *Science* **279**, 1166 (1998).

21. Superpositions based on C $\alpha$  atoms in the platform  $\beta$  strands reveal that the ZAG platform is more similar to classical class I MHC molecules than to any of the class I homologs [rms deviations for superpositions of platforms: ZAG and HLA-A2, 1.3 Å (147 C $\alpha$  atoms); ZAG and CD1, 1.1 Å (86 C $\alpha$  atoms); ZAG and FcRn 1.0 Å (88 C $\alpha$  atoms); ZAG and HFE 1.0 Å (115 C $\alpha$  atoms)].

22. L. M. Sánchez, A. J. Chirino, P. J. Bjorkman, G. Hathaway, P. G. Green, K. Faull, unpublished results.

23. Figures 1, 2A (right), 2B, 3A, and 3C were made using MOLSCRIPT [P. J. Kraulis, *J. Appl. Crystallogr.* **24**, 946 (1991)] and RASTER-3D [E. A. Merritt and M. E. P. Murphy, *Acta Crystallogr. D* **50**, 869 (1994)]. Electrostatic calculations were done and Figs. 2A (left) and 3B were made using GRASP [A. Nicholls, R. Bharadwaj, B. Honig, *Biophys. J.* **64**, A166 (1993)].

24. ZAG, CD1, HFE, and FcRn contain prolines within their  $\alpha$ 2 domain helices at a position corresponding to Val<sup>165</sup> in classical class I MHC molecules (4). The FcRn and CD1 helices are kinked at a position near their proline residues, whereas the ZAG and HFE helices are similar to the  $\alpha$ 2 domain helices of class I molecules (71). Substitution of Val<sup>165</sup> for proline in the mouse class I molecule H-2D<sup>d</sup> did not interfere with binding and presentation of peptides to T cells, suggesting that no major structural rearrangements occurred [D. Plaksin, K. Polakova, M. G. Mage, D. H. Margulies, *J. Immunol.* **159**, 4408 (1997)].

25. We thank G. Hathaway, P. G. Green, and K. Faull for mass spectrometric analyses. ZAG coordinates have been deposited in the PDB (code 1zag). L.M.S. was supported by a grant from the U.S. Department of Defense Breast Cancer Research Program.

21 December 1998; accepted 18 February 1999

## News Releases

April 28, 1999

### Caltech biologists reveal structure of protein responsible for weight loss in cancer and AIDS patients

PASADENA-Caltech biologists have determined the three-dimensional structure of a protein that causes wasting in cancer and AIDS patients. The discovery could lead to new strategies for controlling weight loss in patients with devastating illnesses-and conversely, perhaps new strategies for fighting obesity.

The protein is commonly known as ZAG and is found in most bodily fluids. But researchers have been aware for some time that the protein is particularly abundant in patients who have cancer.

More recently, researchers have discovered that the protein is involved in the wasting syndrome known as cachexia, which is associated with both cancer and AIDS.

"This protein has something to do with fat metabolism," says Pamela Bjorkman, a professor of biology at Caltech and associate investigator of the Howard Hughes Medical Institute. Bjorkman and her team recently published a paper in the journal *Science* showing ZAG's structure.

One of the most noteworthy features of the structure is the resemblance between ZAG and a family of proteins known as class I major histocompatibility complex molecules, or MHC.

"MHC proteins have a large groove that binds a peptide derived from a pathogen," says Bjorkman, explaining that their new picture of the ZAG crystal shows an unexpected blob in the ZAG counterpart of the MHC peptide binding groove.

"It's not a peptide, but some organic molecule," she says. "We suspect that it is involved in the function of ZAG. If this compound is involved in breaking down lipids, then maybe you could design a drug that replaces it and interfere with lipid breakdown."

According to Bjorkman, other research shows that tumor cells themselves seem to stimulate the body to overproduce ZAG somehow, which in turn leads to the breakdown of body fat.

Thus, people suffering from cachexia don't lose body weight because they don't eat, but because the fat in their bodies is ultimately destroyed by an interaction involving ZAG.



Human ZAG

Three-dimensional structure of a human ZAG.

#### Related Links

[Dr. Pamela Bjorkman](#)

[Science](#)

[Howard Hughes Medical Institute](#)

An intervention to stop the wasting, then, might be to disrupt the overexpression of ZAG, and this might be accomplished with monoclonal antibodies or small molecules that bind to ZAG, she says.

The research appeared in the March 19 issue of *Science*, and was also the subject of an article in HHMI news, published by the Howard Hughes Medical Institute.

The other authors of the paper are Luis Sanchez and Arthur Chirino, both senior research fellows in Bjorkman's lab.

Contact: Robert Tindol (626) 395-3631 [tindol@caltech.edu](mailto:tindol@caltech.edu)

---

***Navigating Tools***

Search:  in

Choose Destination:



Email us at [prmedia@caltech.edu](mailto:prmedia@caltech.edu) with comments, questions or suggestions.

## Structure of Fat-Depleting Protein Reveals Important Functional Clues

### *In the Groove*

Finding a molecule that binds in ZAG's (red) groove may yield the template for a new class of obesity drugs.

**news archive**  
**info for reporters**  
**annual report**  
**HHMI news**  
**HHMI home**

Download this story  
in Acrobat PDF  
format.  
(requires Acrobat  
Reader)

**HHMI Research  
News Updates:**  
If you'd like to receive  
email notification of  
breaking HHMI  
research news, please  
enter your email  
address and click the  
send button.



*March 19, 1999—*  
Following a mysterious crevice in a molecule that causes severe weight loss in some cancer patients may turn up a new generation of drugs to treat clinical obesity, say researchers from the Howard Hughes Medical Institute (HHMI) at the California Institute of Technology.

Zn- $\alpha$ 2-glycoprotein, otherwise known as ZAG, occurs naturally

in most body fluids, including blood, sweat, saliva, and urine. Researchers first isolated ZAG from blood samples more than 30 years ago, "but it's been a molecule in search of a function for a long time," said Pamela Bjorkman, an HHMI investigator at the California Institute of Technology in Pasadena. Bjorkman, Luis Sánchez and HHMI associate Arthur Chirino published ZAG's structure in the March 19, 1999, issue of the journal *Science*.

One of the mysteries surrounding ZAG is that it seems to be related to a large family of proteins known as class I major histocompatibility complex (MHC) molecules. These molecules bind to small pieces of other proteins, known as antigenic peptides, and in so doing trigger an immune response to invading microorganisms and viruses. Yet despite ZAG's similarity to MHC proteins, it apparently does not have a role in the immune system, Bjorkman said.

Last year, however, researchers at Aston University in Birmingham, U.K., discovered that ZAG is involved in cachexia, a wasting syndrome that can affect people

with cancer, AIDS and other terminal illnesses. Cachexia can result in rapid, life-threatening weight loss and lead to shedding of both fat and muscle.

ZAG appears to drive the fat-loss in cancer patients. When the British investigators added ZAG to fat cells, the cells rapidly metabolized lipids, a major component of fat. Further evidence of ZAG's role in fat breakdown came when researchers, who fed the protein to genetically obese mice, noticed that the mice lost body fat even though they maintained normal eating habits. If ZAG produces the same effect in humans and is deemed safe, Bjorkman adds, it could provide a long-sought treatment for clinical obesity.

Understanding how ZAG boosts fat breakdown is a necessary precursor to any plans to develop ZAG-based obesity drugs. Knowing that structure often reveals details about function, Bjorkman's group created a molecular map of ZAG's structure using x-ray crystallography, which provides a three-dimensional picture revealing the location of each of the molecule's atoms. Surprisingly, this image showed that ZAG's structure is even more like that of its MHC relatives than researchers had previously thought.

One distinguishing feature of MHC proteins is a large groove that the molecules use to bind antigenic peptides. Bjorkman's group discovered that ZAG also has this groove, but unlike MHC molecules, ZAG's groove doesn't bind peptides. "We found that the ZAG groove contains some sort of compound. We know that it's not a peptide, but we haven't identified it yet," Bjorkman said. A search of small molecule databases for molecules capable of fitting in the groove failed to find any good candidates among known compounds.

Bjorkman's top priority is to find the molecule that binds in ZAG's groove, since this unknown partner may hold the key to understanding how ZAG promotes fat breakdown. "There's a big hint there," said Bjorkman, "we just don't know what the answer is yet. But once we identify this compound, it's possible you could inhibit the binding of this molecule to ZAG as a treatment for cachexia." She added that such a strategy might be particularly helpful for breast cancer patients since ZAG accumulates in 40 percent of cancerous breast tissue.

The information about ZAG's structure also provides important clues about the evolution of the MHC protein family. Bjorkman explained that prior to this and other structural work on MHC-related proteins, researchers believed that the MHC molecule groove evolved to bind

antigenic peptides. Given the fact that ZAG shares this structure yet is not involved in the immune system suggests that the groove may have evolved for a different reason, she says.

"Perhaps the groove first evolved for a purpose other than antigen binding and MHC molecules have just capitalized on its existence," said Bjorkman. "But there's still a lot we don't understand." Determining ZAG's structure, she added, is simply the first step towards understanding how the molecule does its job.

illustration: Pamela Bjorkman



Top of Page...

[HHMI Home](#) | [Research](#) | [Grants](#) | [Publications](#) | [Jobs](#) | [News](#) | [Search](#)